Available online at www.sciencedirect.com
SCIENCE DIRECT
Polymer 46 (2005) 12046–12056
polymer
www.elsevier.com/locate/polymer

Mechanism and kinetics of the free radical ring-opening polymerization of cyclic allylic sulfide lactones

Marisa Phelan [a], Fawaz Aldabbagh [a,*], Per B. Zetterlund [b], Bunichiro Yamada [a]

[a] *Department of Chemistry, National University of Ireland, Galway, Ireland*
[b] *Graduate School of Science and Technology, Kobe University, Kobe 657-8501, Japan*

Received 16 August 2005; received in revised form 20 October 2005; accepted 1 November 2005

Abstract

The polymerization of 7-, 8- and 11-membered lactones, 6-methylene-1,4-oxathiepan-7-one, 3-methylene-1,5-oxathiocan-2-one and 3-methylene-1-oxa-5-thiacycloundecan-2-one in benzene at 70, 40–70 and 40–65 °C, respectively, is presented. All polymerizations proceeded with complete ring-opening up to approximately 25% conversion, where insoluble polymer was formed. Evidence is given attributing polymer double bond loss to crosslinking, although redistribution of the molecular weights via addition to polymer double bonds followed by β-fragmentation also appears to occur for polymerizations of the 8- and 11-membered lactones. Michael adducts of lactones with 2-methyl-2-propanethiol were prepared as models for chain-transfer products of hydrogen abstraction by carbon-centred radicals. Polymerization rates were found to increase marginally with ring size. Arrhenius parameters obtained for the polymerizations of the 8- and 11-membered lactones indicated that the addition step was more important than fragmentation in determining the rate of propagation.

Keywords: Radical polymerization; Ring-opening; Sulfur

1. Introduction

The free radical ring-opening of cyclic monomers is important since it allows the introduction of various functional groups into polymer backbones by chain growth rather than step-growth polymerization, and smaller volume shrinkage is often achieved in comparison to non-cyclic and/or vinyl monomer polymerizations [1]. In the mid-1990s the Australian CSIRO group introduced two new classes of cyclic allylic sulfur-containing ring-opening monomers (Fig. 1). For both classes, ring-opening gave propagating sulfur-centred radicals and generation of polymer backbone double bonds. The advantage of sulfur-centred propagating radicals in comparison to more common oxygen and carbon-centred propagating radicals is the negligible chain transfer by hydrogen abstraction. The first class were 7- to 13-membered cyclic structures containing an acrylate functional group of which lactone monomers 6-methylene-1,4-oxathiepan-7-one **1**, 5-methyl-6-methylene-1,4-oxathiepan-7-one **2** and 3-methylene-1-oxa-5-thiacycloundecan-2-one **4** are examples [2,3]. The second were disulfide monomers [4–6] of which the 8-membered monomer 2-methyl-7-methylene-1,5-dithiocane **5** has been thoroughly studied with NMR analysis of the resultant homo- and co-polymer backbones [4–7], copolymerization [7,8], chain transfer [9–11] and propagation-depropagation [12] kinetics and mechanisms presented.

In comparison very little research has been published on the lactone monomers with CSIRO reporting several polymerizations of **1**, **2** and **4** using monomer or comonomer concentrations of 3 M in benzene at 70 °C [2,3]. Homopolymerization and copolymerization of **1** with methyl acrylate and styrene (St) were found to be difficult because of the ready formation of insoluble gels. It seemed that the activated double bond of the polymer backbone was susceptible to radical attack leading to crosslinking. However, copolymerization up to high conversion of **1** with 5 equivalents of methyl methacrylate (MMA) produced soluble polymer presumably because of steric restraints of the methyl substituent of MMA reducing crosslinking. The reactivity of the acrylate or lactone monomers was similar to that of MMA resulting in copolymer compositions similar to that of the feed. The exception was **2**, which was found to be less reactive

* Corresponding author. Tel.: +353 91 524411; fax: +353 91 525700.
E-mail addresses: fawaz.aldabbagh@nuigalway.ie (F. Aldabbagh), pbzttlnd@cx6.scitec.kobe-u.ac.jp (P.B. Zetterlund), bunich@mail.goo.ne.jp (B. Yamada).

0032-3861/$ - see front matter © 2005 Elsevier Ltd. All rights reserved.
doi:10.1016/j.polymer.2005.11.006

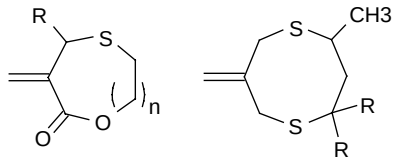

1: (R = H, n = 1)
2: (R = CH_3, n = 1)
3: (R = H, n = 2)
4: (R = H, n = 5)

5: (R = H)
6: (R = CH_3)

Fig. 1. Lactone monomers **1**–**4** and disulfide monomers **5**–**6**.

presumably because of the methyl substituent at the allylic position, which also reduced the level of crosslinking and thus gel formation. Homopolymerization and copolymerizations of **2** with St gave soluble polymers. Chaumont et al. examined the base hydrolysis of the ester functional groups of copolymers of **1** and **2** with St allowing the formation of degradable materials [13]. The decrease in the molecular weight upon hydrolysis was smaller than expected based on the number of hydrolysed groups, which was attributed to formation of saturated esters via chain transfer or crosslinking reactions.

Scheme 1 outlines the two-step mechanism of propagation for the lactone monomers. The first step involves the addition of a sulfanyl radical onto the monomer double bond to form the intermediate carbon centred radical **7**. The second step involves fragmentation of **7** to yield a new propagating sulfanyl radical and polymer backbone double bond.

In the present paper, we report the first detailed homopolymerization studies of the lactone monomers, which were carried out at a lower monomer concentration ([*M*] = 2 M) than polymerizations reported by the CSIRO in order to minimize insoluble polymer formation [2,3]. The level of double bond loss leading to crosslinking was determined by NMR. The influence of ring size on the polymerization rates of 7-membered **1**, new 8-membered, 3-methylene-1,5-oxathiocan-2-one **3** and 11-membered **4** lactone monomers is presented. Michael additions of 2-methyl-2-propanethiol onto **1** and **3** have been carried out in order to obtain model compounds for the products of chain transfer. Values for the lumped parameter $k_p/k_t^{0.5}$ (where k_p and k_t are the rate coefficients for propagation and termination, respectively) were determined for **3** and **4** as a function of temperature. Examination of the Arrhenius parameters allowed assessment of the relative importance of the two steps in Scheme 1 in determining the propagation rate. Comparisons are made with disulfides **5** and 2,2,4-trimethyl-7-methylene-1,5-dithiocane **6** [12].

2. Experimental

2.1. Materials

Initiators were purchased commercially; 2,2′-azo(isobutyronitrile) (AIBN) from DuPont Chemical Solution Enterprise, and was re-crystallized using methanol before use and *tert*-butyl peroxide (TBP) from Aldrich was used as purchased. Thin layer chromatography and column chromatography were carried out using aluminum-backed plates coated with silica gel (Merck $60F_{254}$) and Merck Isabel 60H silica, respectively. All other chemicals used were purchased from Aldrich.

2.2. Characterization

Melting points were measured on a Stuart Scientific melting point apparatus SMP3. IR spectra were acquired using a Perkin–Elmer Spec 1 with ATR attached. All ^1H and ^{13}C NMR spectra were recorded in $CDCl_3$ at 400 and 100 MHz, respectively, using a Jeol GXFT 400 MHz instrument equipped with a DEC AXP 300 computer work station. NMR assignments were supported by HMQC (Heteronuclear Multiple Quantum Correlation) ^1H-^{13}C 2D spectra, and DEPT (distortionless enhancement through polarization transfer). EPSRC National Mass Spectrometry Service Centre, University of Wales, Swansea carried out low resolution electron impact (EI)

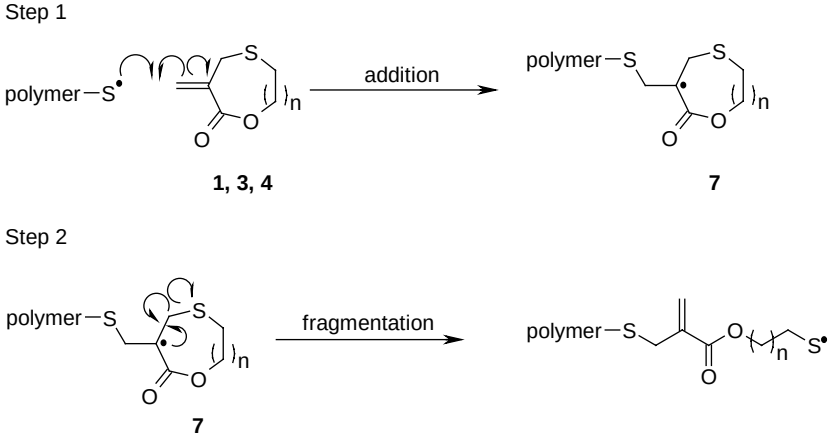

Scheme 1. Two-step ring-opening polymerization mechanism for **1** (n = 1), **3** (n = 2) and **4** (n = 5).

on the Micromass Quattro II triple quadrupole instrument (EI source temperature 200 °C and electron energy 70 eV) and high-resolution mass spectrometry on the Finnigan MAT 900 XLT in chemical ionization (CI) mode (CI source temperature ca. 140 °C and electron energy 200 eV).

2.3. Preparation of monomers

Monomers **1** and **4** were prepared according to the CSIRO international patent [2]. Monomer **3** was prepared using a similar procedure:

Triethylamine (10 ml, 0.07 mol) was added over 30 min to α-(bromomethyl)acrylic acid [2] (5.70 g, 0.04 mol) in CH_2Cl_2 (150 ml) on an ice-bath. 3-Mercapto-1-propanol (3.21 g, 0.04 mol) was added over a period of 15 min, and the reaction mixture was stirred at room temperature for 18 h. The reaction mixture was added to ammonium sulfate (16 g, 0.12 mol) and 2 M sulfuric acid (5 ml) in water (50 ml). After a period of 10 min a white precipitate was observed and the mixture was extracted with diethyl ether (3×60 ml), dried ($MgSO_4$) and evaporated to dryness. The residue was purified by re-crystallisation (ethyl acetate/hexane 1:1) to yield α-{[(3-hydroxypropyl)thio]methyl}acrylic acid (3.89 g, 64%), as a cream solid; mp 69–71 °C; IR (neat) 3106, 2933, 2886, 2620, 1706 (C=O), 1676, 1620, 1436, 1310, 1213, 1200, 1136, 1043, 970, 910 cm^{-1}; δ_H 1.81–1.87 (m, 2H, SCH_2CH_2), 2.60 (t, 2H, $J=7.1$ Hz, SCH_2CH_2), 3.39 (s, 2H, allylic-CH_2), 3.75 (t, 2H, $J=6.0$ Hz, CH_2OH), 5.77 (s, 1H, $=CH_2$), 6.33 (s, 1H, $=CH_2$), OH signals not observed; δ_C 28.4 (CH_2S), 31.6 (SCH_2CH_2), 32.5 (allylic-CH_2), 61.7 (CH_2OH), 128.3 ($=CH_2$), 136.2 (=C), 170.4 (C=O).

A solution of α-{[(3-hydroxypropyl)thio]methyl}acrylic acid (3.0 g, 0.02 mol) and triethylamine (19 ml, 0.14 mol) in CH_2Cl_2 (60 ml) was added by syringe pump to a refluxing solution of 2-chloro-1-methylpyridinium iodide (17.0 g, 0.07 mol) in CH_2Cl_2 (800 ml) over a period of 8 h. The solution was allowed to reflux for a further 2 h, filtered and evaporated to give viscous light brown slurry. Water (100 ml) was added and the mixture extracted with CH_2Cl_2 (3×60 ml). The organic extracts were dried ($MgSO_4$) and evaporated to dryness. The residue was purified by column chromatography using silica gel as absorbent and CH_2Cl_2 as eluent to yield **3** (1.8 g, 68%), as colorless crystals, mp 18–19 °C. (Found $M+NH_4^+$, 176.0740. $C_7H_{14}NO_2S$ requires $M+NH_4^+$ 176.0740); IR (neat) 2960, 2915, 1728 (C=O), 1643, 1462, 1419, 1372, 1291, 1271, 1160, 1136, 1069, 1036; δ_H 1.92–2.01 (m, 2H, 7-CH_2), 2.61–2.67 (m, 2H, 6-CH_2), 3.37 (s, 2H, allylic-CH_2), 4.28 (t, 2H, $J=6.1$ Hz, OCH_2), 5.25 (s, 1H, $=CH_2$), 5.61 (s, 1H, $=CH_2$); δ_C 31.7 (6-CH_2), 32.7 (7-CH_2), 38.8 (allylic-CH_2), 69.5 (OCH_2), 120.8 ($=CH_2$), 141.2 (=C), 169.9 (C=O); *m/z* (EI) 158 (M^+, 100%), 130 (91), 100 (80).

2.4. Michael additions

A solution of **1** (0.20 g, 1.4 mmol) and 2-methyl-2-propanethiol (0.08 g, 0.9 mmol) in diethyl ether (50 ml) was added to a solution of sodium hydride (0.05 g, 0.2 mmol) in diethyl ether (50 ml) and allowed to stir at room temperature for 2 h (Scheme 2). The solution was filtered and evaporated to give a residue, which was purified by column chromatography using silica gel as absorbent and CH_2Cl_2 as eluent to yield 6-[(*tert*-butylthio)methyl]-1,4-oxathiepan-7-one **8** (0.09 g, 42%), as a clear solid, mp 42–43 °C. (Found MH^+, 235.0819. $C_{10}H_{19}O_2S_2$ requires MH^+ 235.0821); IR (neat) 2960, 2900, 2860, 1730 (C=O), 1456, 1363, 1153, 910 cm^{-1}; δ_H 1.35 (s, 9H, CH_3), 2.70–2.99 (m, 7H, 1-CH_2, CH, CH_2SCH_2), 4.29–4.31 (m, 2H, OCH_2); δ_C 29.4 (CH_2), 29.7 (CH_2), 31.0 (CH_3), 33.3 (CH_2), 42.8 (C–S), 46.5 (CH), 63.7 (OCH_2), 172.6 (C=O); *m/z* (EI) 215 (10%), 158 (22), 121 (21), 91 (60), 73 (58), 41 (100).

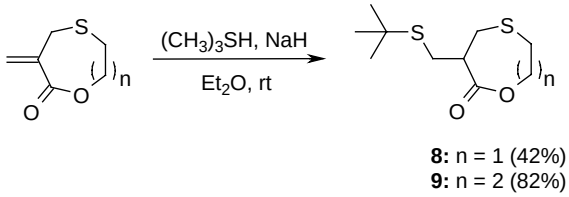

Scheme 2. Michael additions of 2-methyl-2-propanethiol onto **1** (n=1) and **3** (n=2).

The procedure for preparation of 3-[(*tert*-butylthio) methyl]-1,5-oxathiocan-2-one **9** is as for **8**; **3** (0.20 g, 1.3 mmol), 2-methyl-2-propanethiol (0.08 g, 0.9 mmol) and sodium hydride (0.05 g, 0.2 mmol) gave **9** (0.17 g, 82%), as a white solid, mp 47–48 °C. (Found MH^+, 249.0977. $C_{11}H_{21}O_2S_2$ requires MH^+249.0977); IR (neat) 2953, 2920, 2860, 1740 (C=O), 1456, 1363, 1276, 1153, 1006 cm^{-1}; δ_H 1.29 (s, 9H, CH_3), 2.05–2.14 (m, 2H, SCH_2CH_2), 2.55–2.68 (m, 3H, 4-C*H*H, 6-CH_2), 2.79–2.85 (m, 1H, CH), 2.91–3.02 (m, 2H, 4-C*H*H, 1-CH*H*), 3.10–3.15 (m, 1H, 1-C*H*H), 4.02–4.16 (m, 1H, OCH_2), 4.52–4.66 (m, 1H, OCH_2); δ_C 27.5 (4-CH_2), 31.0 (CH_3), 31.8 (6-CH_2), 32.7 (7-CH_2), 39.9 (*tert*-Bu-SCH_2), 42.6 (C-S), 46.2 (CH), 64.5 (OCH_2), 175.4 (C=O); *m/z* (EI) 248 (M^+, 20%), 191 (64), 149 (24), 105 (39), 73 (33), 57 (100), 51 (54).

2.5. Polymerization procedures

All polymerizations were carried out in Pyrex glass ampoules, degassed with several freeze-thaw cycles, sealed under vacuum and heated for the prescribed times in an aluminium heating mantel at the required temperature. Polymerization solutions contained 2 M of **1**, **3** or **4**, with initiator in benzene. Polymerizations of **1** at 70 °C used 0.02 M AIBN. Polymerization of **3** at 40, 50, 60, 65 and 70 °C used 0.30, 0.08, 0.05, 0.02 and 0.02 M of AIBN, respectively. Polymerization of **4** at 40, 50, 60 and 65 °C used 0.350, 0.200, 0.025 and 0.010 M of AIBN, respectively. After the polymerizations, the ampoules were rapidly cooled in an ice-water bath, benzene was removed under vacuum and the samples dissolved in $CDCl_3$ for estimation of conversion by ^1H NMR. Samples used for characterization of polymers **1**, **3** and **4**

by NMR were dissolved in CH_2Cl_2 and precipitated from methanol.

2.6. Polymerization measurements

The conversions for the polymerizations of **1**, **3** and **4** were measured from the decrease in the area of the monomer vinyl proton at 5.55, 5.25 and 5.50 ppm, respectively, after normalization with respect to the integration area of the entire ^{1}H NMR spectrum.

Estimation of the double bond loss during the polymerization was carried out using ^{1}H NMR by dividing the total area of the vinyl region (5.2–6.6 ppm) of the polymerization mixture containing monomer and polymer by the vinyl region of the monomer before polymerization, after normalization of both spectra to the integration area of the entire spectrum.

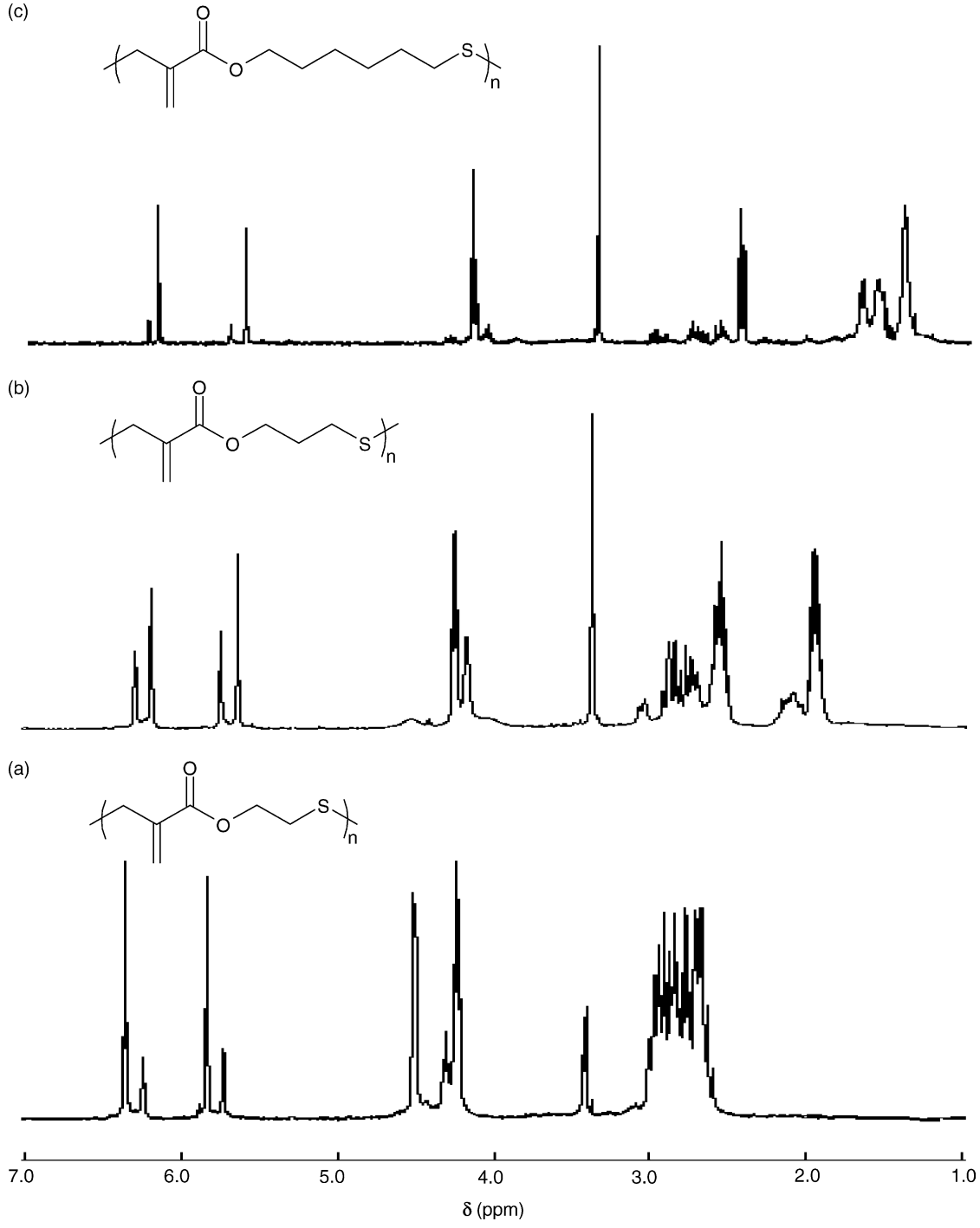

Fig. 2. ^{1}H NMR spectra of the precipitated polymers of the polymerization of 2 M benzene solutions of (a) monomers **1**, $[AIBN]_0 = 0.02$ M, after 1 h at 70 °C resulting in poly(**1**) in 17% conversion, (b) **3**, $[AIBN]_0 = 0.05$ M, after 2 h at 60 °C resulting in poly(**3**) in 18% conversion, (c) **4**, $[AIBN]_0 = 0.010$ M, after 1 h at 65 °C resulting in poly(**4**) in 12% conversion.

Molecular weights were measured by a Viscotek GPC system equipped with a Viscotek DM 400 Data Manager, a Viscotek VE 3580 RI detector and a Viscotek Viscogel column GMHHR-M. THF was used as eluent at a flow rate of 1.0 mL min^{-1}. Poly(St) standards (M_n = 376–2,570,000) were used for calibration.

2.7. Characterization of polymers

2.7.1. Poly(*1*)

Polymerization of **1** for 1 h at 70 °C resulted in 17% conversion, M_n = 9100, M_w/M_n = 1.75; IR ($CHCl_3$) 2947, 2924, 1745 (adjacent to crosslink, C=O), 1713 (α, β-unsaturated C=O), 1456, 1295, 1137 cm^{-1}; δ_H 2.59–3.03 (m, CH_2S), 3.37 (minor, m, allylic-CH_2), 4.23 (t, J = 6.8 Hz, OCH_2), 4.30 (minor, t, J = 6.7 Hz, OCH_2), 4.47–4.54 (m, OCH_2), 5.73 (minor, s, =C*H*H), 5.84 (s, =C*H*H), 6.24 (minor, s, =C*H*H), 6.35 (s, =C*H*H) (Fig. 2(a)). Minor peaks at 3.37, 4.30, 5.73, and 6.24 ppm in the ^1H NMR spectrum are approximately 30% relative to the intensity of the major polymer repeat unit represented by $=CH_2$ peaks at 5.84 and 6.35 ppm; δ_C 26.3, 29.5, 32.1, 32.3, 32.7, 35.6, 35.8, 36.6, 37.8 (all CH_2S), 55.9 (q-C, crosslink), 63.5 (minor, OCH_2), 64.0 (OCH_2), 72.4 (OCH_2), 127.2 (minor, $=CH_2$), 130.7 ($=CH_2$), 135.3 (=C), 136.4 (minor, =C), 165.7 (minor, α, β-unsaturated C=O), 166.5 (α, β-unsaturated C=O), 178.3 (C=O adjacent to crosslink) (Fig. 3(a)).

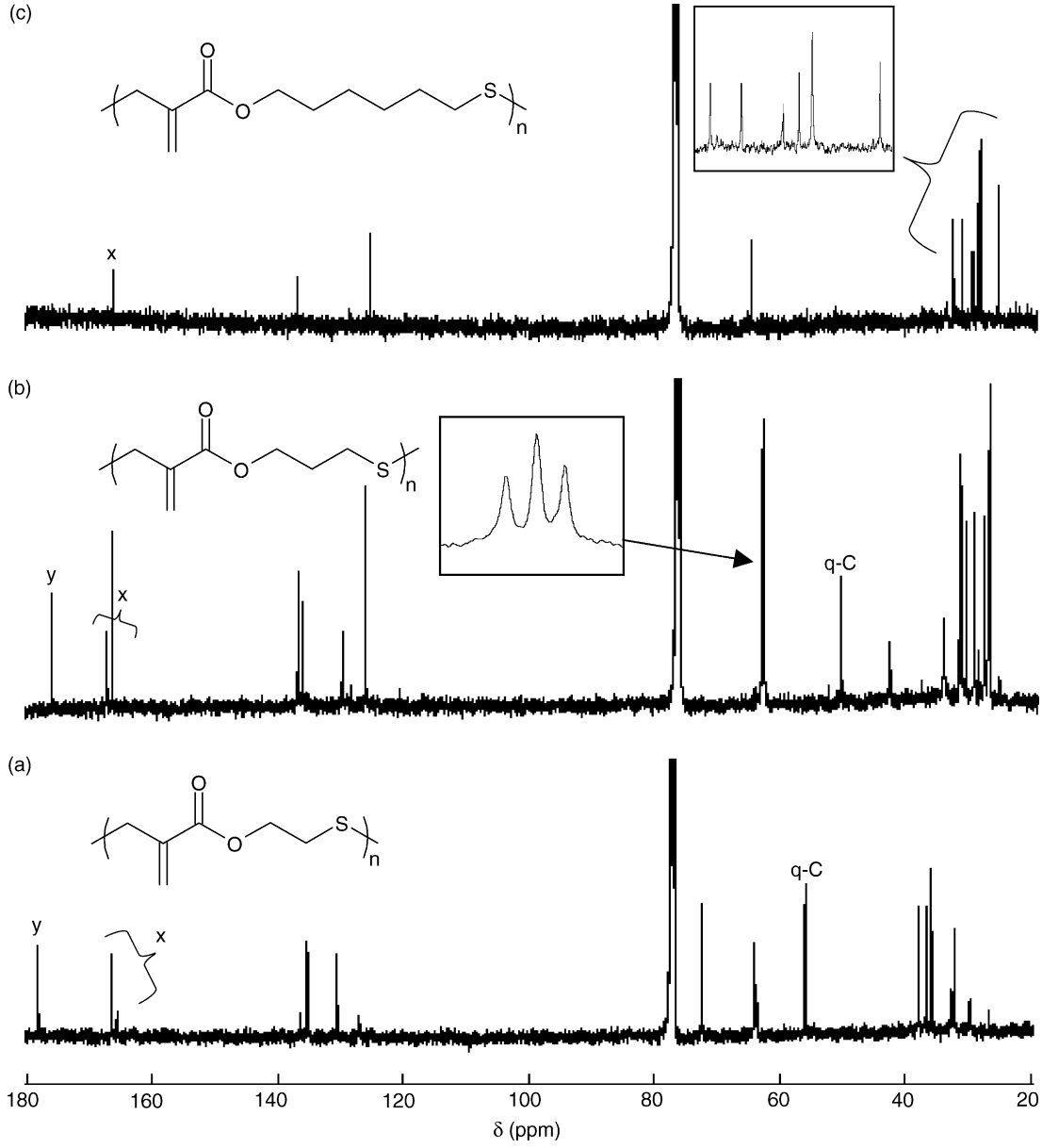

Fig. 3. ^{13}C NMR spectra of the precipitated polymers shown in Fig. 2 of (a) poly(**1**), (b) poly(**3**) and (c) poly(**4**), where q-C is a crosslinked carbon, x and y are α, β-unsaturated C=O and C=O adjacent to a crosslink, respectively.

*2.7.2. Poly(**3**)*

Polymerization of **3** for 2 h at 60 °C resulted in 18% conversion, $M_n = 19{,}200$, $M_w/M_n = 3.08$; IR (neat) 2970, 2906, 1733 (adjacent to crosslink, C=O), 1715 (α, β-unsaturated C=O), 1409, 1256, 1133, 1050 cm^{-1}; δ_H 1.88–1.98 (m, CH_2CH_2S), 2.03–2.16 (minor, m, CH_2CH_2S), 2.45–2.62 (m, CH_2S), 2.68–2.96 (m, CH_2S), 3.03–3.10 (minor, m, CH_2S), 3.37 (s, allylic-CH_2), 4.10–4.17 (m, OCH_2), 4.25 (t, $J = 6.2$ Hz, OCH_2), 4.54 (minor, broad-s, OCH_2), 5.64 (s, =C*H*H), 5.75 (minor, s, =C*H*H), 6.19 (d, $J = 4.3$ Hz, =C*H*H), 6.29 (minor, d, $J = 3.4$ Hz, =C*H*H) (Fig. 2(b)). Minor peaks at 2.03–2.16, 5.75 and 6.29 ppm in the ^{1}H NMR spectrum are approximately 60% relative to the intensity of the major polymer repeat unit represented by $=CH_2$ peaks at 5.64 and 6.19 ppm; δ_C 28.0, 28.1, 28.2, 28.4, 28.9, 29.8, 30.5, 31.8, 32.5, 32.8, 32.8, 35.3, 43.8 (all CH_2), 51.4 (q-C, crosslink), 63.6, 63.7, 63.9 (all OCH_2), 126.2 ($=CH_2$), 129.8 ($=CH_2$), 136.0 (=C), 136.8 (=C), 166.1 (α, β-unsaturated C=O), 166.9 (minor, α, β-unsaturated C=O), 175.5 (C=O adjacent to crosslink) (Fig. 3(b)).

*2.7.3. Poly(**4**)*

Polymerizations of **4** for 1 h at 65 °C resulted in 12% conversion, $M_n = 26{,}300$, $M_w/M_n = 1.38$; IR (neat): 2920, 2852, 1710 (α, β-unsaturated C=O), 1456, 1325, 1302, 1182, 1128 cm^{-1}; δ_H 1.34–1.45 (m, CH_2), 1.58–1.61 (m, CH_2), 1.64–1.71 (m, CH_2), 2.44 (t, $J = 7.2$ Hz, CH_2S), 2.53–2.61 (minor, m, CH_2), 2.66–2.80 (minor, m, CH_2), 2.93–3.02 (minor, m, CH_2), 3.36 (s, allylic-CH_2), 4.05–4.08 (minor, m, OCH_2), 4.16 (t, $J = 6.7$ Hz, OCH_2), 4.28–4.34 (minor, m, OCH_2), 5.62 (s, =C*H*H), 5.72 (minor, s, =C*H*H), 6.18 (s, =C*H*H), 6.24 (minor, s, =C*H*H) (Fig. 2(c)); minor peaks at 5.72, and 6.24 ppm in the ^{1}H NMR spectrum are approximately 25% relative to the intensity of the major polymer repeat unit represented by $=CH_2$ peaks at 5.62 and 6.18 ppm. δ_C 25.7 (CH_2), 28.6 (CH_2), 29.1 (CH_2), 29.8 (CH_2), 31.6 (allylic-CH_2), 32.9 (CH_2S), 65.1 (OCH_2), 125.7 ($=CH_2$), 137.1 (=C), 166.6 (C=O) (Fig. 3(c)).

3. Results and discussion

3.1. Interpretation of NMR spectra of polymers

The addition of two possible radicals onto polymer backbone double bonds can occur; cyclic carbon-centred adduct radicals **7** formed in step 1 of the mechanism (Scheme 1) or propagating sulfanyl radicals (both labelled $P_n^\bullet$ in Scheme 3). The addition of $P_n^\bullet$ gives carbon-centred adduct radical **10** which can form a crosslink by either addition to monomer, which leads to propagation, or via bimolecular termination of propagating radicals with **10**. The crosslinks result in additional non-equivalent signals in the NMR spectra. Alternatively, **10** can undergo β-fragmentation leading to the formation of a new propagating polymeric sulfanyl radical ($P_mS^\bullet$) (Scheme 3) [11]. This intermolecular chain transfer, as well as intramolecular backbiting followed by fragmentation [9] have no effect on overall double bond content (Section 3.2).

Monitoring of the total double bond content by ^{1}H NMR showed that poly(**4**) in Fig. 2(c) had undergone only ≈1% loss of polymer backbone double bonds (Section 3.2). The poly(**4**)

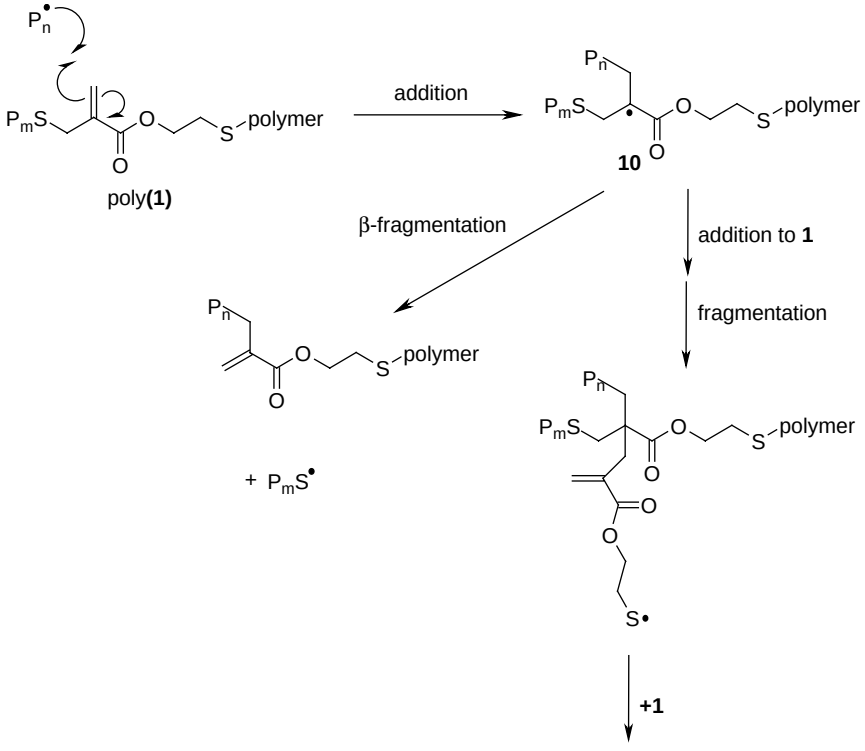

Scheme 3. Mechanism showing radical addition onto poly(**1**) backbone double bond followed by β-fragmentation or crosslinking of the carbon-centred adduct radical **10**.

spectrum in comparison to the other precipitated polymer samples of **1** (Fig. 2(a)) and **3** (Fig. 2(b)) is more well-defined and *J*-values were obtained for the OCH_2 and CH_2S signals (Section 2.7). Some additional minor complex multiplets (2.53–3.02, 4.05–4.08 and 4.28–4.34 ppm) and vinyl peaks (≈25% of the intensity of the major vinyl peaks) were obtained (Fig. 2(c)) indicating that the polymer did contain some additional minor chemically non-equivalent parts. Additional signals did not appear in the ^{13}C NMR spectrum (Fig. 3(c)), as only 10 carbon signals equivalent to the ring-opened polymer (Scheme 1) unit were observed.

The precipitated polymers of **1** and **3** had undergone more significant double bond loss compared to **4** with 17 and 4% loss (Section 3.2). In both ^1H NMR spectra (Fig. 2(a) and (b)) the additional minor non-equivalent signals are of a greater intensity than in poly(**4**). The corresponding ^{13}C NMR spectra are much more complex with a large number of CH_2 signals between 26.3–37.8 and 28.0–43.8 ppm for poly(**1**) and poly(**3**) respectively, indicating non-equivalent repeating units in the polymer backbones (Fig. 3(a) and (b)). The three signals at 63.5 (minor), 64.0 and 72.4 ppm for poly(**1**) and the three lines at 63.6–63.9 ppm for poly(**3**) were assigned as OCH_2 using ^1H-^{13}C HMQC. The vinyl signals in the ^{13}C NMR spectra also correlated to the vinyl signals in the ^1H NMR spectra using ^1H-^{13}C HMQC (Section 2.7). The source of this non-equivalence is attributed to the formation of crosslinks with the quaternary crosslinked carbons detected at 55.9 and 51.4 ppm in the ^{13}C NMR spectrum of poly(**1**) and poly(**3**) respectively. Such a signal was absent in the poly(**4**) ^{13}C NMR spectrum, presumably because of the lower concentration of crosslinks. The chemical shift of the crosslinks is analogous to the structurally similar quaternary carbon at 55.0 ppm formed upon addition-fragmentation cyclization of the chain transfer agent containing two α-(alkylthiomethyl)acryloyloxy groups [14].

The crosslinks resulted in three non-equivalent carbonyl (C=O) signals in the ^{13}C NMR spectra of poly(**1**) and poly(**3**) (Fig. 3(a) and (b)), which is equivalent to the number of OCH_2 signals (see above). The two signals at 165.7, 166.5 and 166.1, 166.9 ppm for poly(**1**) and poly(**3**) respectively, were assigned to α, β-unsaturated carbonyls [14]. The downfield signals at 178.3 and 175.5 ppm for poly(**1**) and poly(**3**) respectively, were assigned to carbonyl (C=O) signals adjacent to the crosslinked carbon [14]. Poly(**4**) gave only one relatively upfield C=O signal at 166.6 ppm assigned to an α, β-unsaturated carbonyl, presumably because of the small amount of double bond loss detected (Section 3.2). Evidence for ester functional groups adjacent to saturated and unsaturated carbon atoms in copolymers of **1** and **2** with St was obtained using IR spectra by Chaumont et al. [13]. The IR spectra we obtained for poly(**1**) and poly(**3**) gave two C=O stretches, which were assigned according to the literature [13], while poly(**4**) gave only one C=O stretch due to the α, β-unsaturated carbonyl consistent with the low level of crosslinking observed in poly(**4**) NMR spectra.

In order to detect chain transfer via hydrogen abstraction by carbon-centred radicals, 2-methyl-2-propanethiol was reacted with **1** and **3** in the presence of sodium hydride (Scheme 2). The novel Michael addition products **8** and **9** were isolated in respective yields of 42 and 82%, and the ^{13}C NMR contained a characteristic CH at ≈46 ppm. However, there were no visible CHs in the polymer spectra, which may rule out hydrogen abstraction by adduct radicals equivalent to **7** or **10** and Michael additions of thiol onto monomer or polymer backbone double bonds as significant reaction pathways.

3.2. Polymer backbone double bonds

The polymerization of **3** and **4** above 70 and 65 °C, respectively, resulted in insoluble polymer after relatively short polymerization times, making kinetic studies at higher temperatures difficult. For example, polymerization of **3** at 70 and 80 °C led to insoluble gel formation after 75 and 30 min using $[AIBN]_0 = 0.02$ M and 0.006 M, respectively. Monomer **4** formed an insoluble gel after 40 and 20 min at 70 and 95 °C using $[AIBN]_0 = 0.02$ M and $[TBP]_0 = 0.02$ M, respectively. For **1**, **3** and **4**, no insoluble polymer was formed at conversions below approximately 25% in the temperature ranges investigated. The polymerization of **1** was carried out only at 70 °C, where considerable loss of polymer backbone double bonds was observed.

The relationship between the formation of insoluble gels and reactions of polymer backbone double bonds may be assessed by monitoring the loss of double bonds by ^1H NMR (Fig. 4). Monomer **1** underwent significant loss of double bonds with 18% loss at 70 °C after 23% conversion (90 min); insoluble polymer had formed at 100 min. Molecular weight distributions (MWD) at different conversion levels are displayed in Fig. 5 for the polymerization of **1** at 70 °C. The

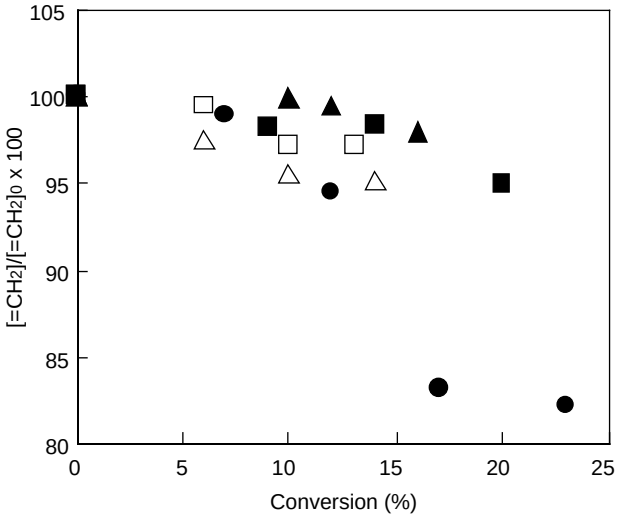

Fig. 4. Total double bond concentration (monomer and polymer), expressed as $[=CH_2]/[=CH_2]_0 \times 100$, where the subscript 0 denotes the initial concentration, vs. conversion (%) for polymerizations of 2 M benzene solutions of **1** at 70 (●) °C, **3** at 40 (□), and 70 (■) °C and **4** at 40 (△) and 65 (▲) °C (selected temperatures shown).

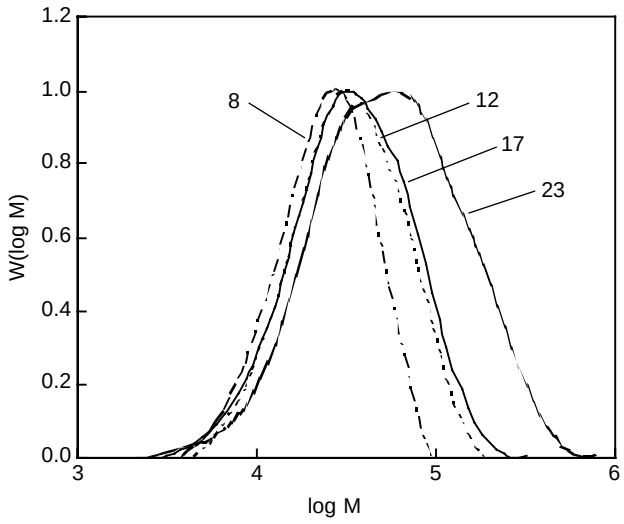

Fig. 5. MWDs for different levels of conversion as indicated (%) for polymerization of 2 M solution of **1** in benzene at 70 °C. Peak heights normalized to unity.

MWDs become broader and shift to higher molecular weights with increasing conversion, consistent with the polymer backbone double bonds being gradually consumed by crosslinking (Scheme 3) as supported by the NMR and IR analyses (Section 3.1).

The double bond loss was much less significant for **3** and **4**, which underwent 5% loss. It is difficult to draw any conclusions with regards to any temperature effect as the extent of loss of double bonds was similar at most temperatures within experimental error (Fig. 4). Broadening of MWD with conversion similar to **1** at 70 °C, but much less pronounced as expected based on the lower extent of loss of polymer backbone double bonds, was also observed for **3** and **4** at the lowest temperature of 40 °C (not shown). However, the trend of broadening of MWD with increasing conversion was not apparent for polymerizations above 40 °C for **3** and **4**. Based on the proposed mechanism of crosslinking (Scheme 3), the extent of crosslinking would be expected to decrease with increasing temperature (under conditions of equal primary chain lengths) due to the higher activation energy of the fragmentation of **10** compared to the activation energy of the addition of monomer to **10** (which leads to crosslinking). Fragmentation of **10** does not lead to crosslinking, but to a redistribution of the polymer chain lengths without any loss of double bonds [11]. However, double bond loss does steadily increase with conversion for all polymerizations.

The rate of formation of insoluble polymer is influenced by a number of factors. The primary chain length plays an important role; the rate of gel formation increases with increasing primary chain length (the rate of crosslink formation per chain increases with increasing chain length, because the number of double bonds per chain is greater for longer chains). M_n of poly(**1**) is significantly lower than M_n of poly(**3**) and poly(**4**) under the current experimental conditions (Table 1), and this would be one reason why **3** and **4** form insoluble polymer at ≈25% conversion, despite undergoing less double bond loss than **1**. Possible reasons for these differences in M_n will be discussed in Section 3.3 in connection with rates of polymerization (R_p).

3.3. Rate of polymerization (R_p) and molecular weights

$R_p/(R_i)^{0.5}$ (i.e. R_p normalized with respect to differences in rate of initiation, R_i) of 7-membered **1** was slightly lower than the 8-membered **3** under identical conditions (Fig. 6). Monomer **4** polymerized faster than **3** at all temperatures (40–65 °C; Table 1), with the greatest difference being approximately a factor of two at 40 °C. Thus, it seems that R_p slightly increase with increasing size of the lactone ring from seven to eleven membered (**1**<**3**<**4**).

R_p may be affected by increasing monomer viscosity [15,16] with increasing ring size at the same monomer concentration (and consequently also higher viscosity of the polymerization mixture). The rate of termination would be anticipated to decrease with increasing monomer viscosity [15,16], consistent with R_p increasing in the order **1**<**3**<**4**.

The amount of crosslinking (Scheme 3) would be also be expected to influence R_p in two opposite ways; higher degrees of crosslinking leads to (i) slower diffusion of propagating radicals, resulting in lower k_t and thus higher R_p [15,17], and (ii) a higher concentration of radical **10** (at the expense of the

Table 1
Polymerizations of 2 M benzene solutions of monomers **1**, **3** and **4**

Monomer	Temperature (°C)	[AIBN] (M)	$R_i \times 10^{7}$[a] (M s^{-1})	$R_p \times 10^{5}$ (M s^{-1})	$R_p/(R_i)^{0.5}$ (M$^{0.5}$ s$^{-0.5}$)	$M_n \times 10^{-3}$ (M_w/M_n)[b]	R_p/R_i
3	40	0.30	1.48	1.91	0.050	59.0 (1.82)	129
4	40	0.35	1.73	4.09	0.098	34.5 (2.31)	236
3	50	0.08	1.67	3.88	0.095	30.8 (2.25)	232
4	50	0.20	4.18	6.37	0.099	32.3 (2.02)	152
3	60	0.05	4.22	6.03	0.093	30.0 (1.67)	143
4	60	0.025	2.11	6.80	0.148	18.1 (1.51)	322
3	65	0.02	4.04	7.50	0.118	21.9 (1.29)	186
4	65	0.01	2.01	6.70	0.150	30.1 (1.30)	334
1	70	0.02	6.34	9.63	0.120	2.5 (2.39)	152
3	70	0.02	6.34	11.75	0.148	15.0 (1.44)	185

[a] Initiator efficiency was assumed to be 0.5.
[b] Conversions are 6–11% in all cases.

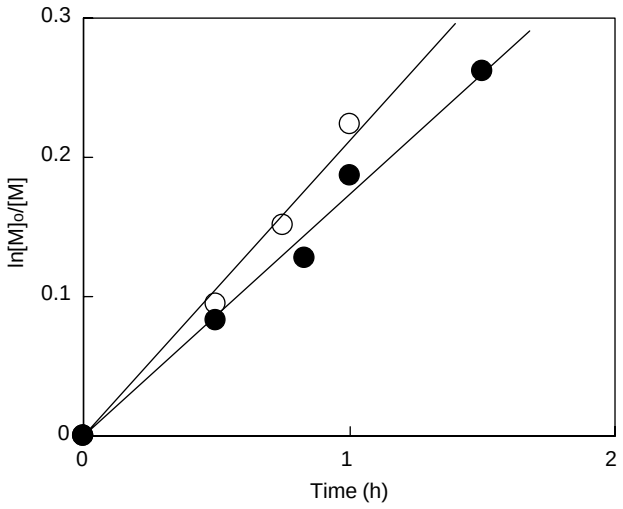

Fig. 6. First-order plot for the polymerization of benzene solutions of **1** (●) and **3** (○) at 70 °C, where $[M]_0=2$ M and $[AIBN]_0=0.02$ M.

propagating sulfanyl radicals), which are expected to propagate more slowly than sulfanyl radicals (primarily because tertiary adduct radicals such as **10** possess a greater amount of steric congestion), and thus lower R_p. The experimental results are consistent with scenario (ii) having a greater impact on R_p since the polymerization of **1**, which resulted in the greatest amount of crosslinks, polymerized the slowest.

For polymerizations of **3** and **4** with similar R_p/R_i, polymers of comparable molecular weight were the result, although no trend between R_p/R_i and M_n was observed (Table 1). Inspection of the entries for R_p/R_i at 65 °C for (**4**), 65 and 70 °C for (**3**) and 70 °C for (**1**) in Table 1 reveals that the significantly lower M_n of poly(**1**) than poly(**3**) and poly(**4**) cannot be explained by differences in R_p/R_i (in the absence of chain transfer, M_n is proportional to R_p/R_i). This suggests that differences in chain transfer rates must be considered. Hydrogen abstraction is known to occur from the allylic position of **1**, as was previously investigated using nitroxide trapping, which resulted in trapping of the conjugated radical at the least hindered position [18]. An increase in steric hindrance with increasing ring size may reduce the level of chain transfer to monomer, and provide an explanation for the lower M_n of **1** in comparison to **3** and **4**. NMR spectra of precipitated polymers of **1**, **3** and **4** showed no evidence of hydrogen abstraction by carbon-centred radicals **7** or **10** (Section 3.1), which infers that propagating sulfanyl radicals may be the cause of chain transfer to monomer despite the weak S–H bond. However, the lack of a CH signal in the ^{13}C NMR spectra of precipitated polymers indicates that the subsequent Michael addition (Scheme 2) involving –SH does not occur to any significant extent. It seems that the allylic hydrogen atoms (two hydrogens in **1**, **3** and **4**, four hydrogens in **5** and **6**) are weakly held due to resonance stabilization of the resultant radical by the double bond allowing usually unreactive radicals in H-abstraction reactions, such as sulfanyl [19,20] and nitroxide radicals [18] to abstract them.

3.4. Arrhenius parameters

First order plots for the polymerization of **3** and **4** are displayed in Figs. 7 and 8, respectively. The values of $k_p/k_t^{0.5}$ were obtained from the slopes $(=(k_p/k_t^{0.5})(fk_d[I]_0)^{0.5})$ assuming an initiator efficiency of 0.5 for AIBN. The quantities $(E_p-0.5E_t)$ and $A_p/A_t^{0.5}$ were subsequently estimated from Arrhenius plots of $k_p/k_t^{0.5}$ (Fig. 9) [12], resulting in $(E_p-0.5E_t)=28$ and 18 kJ mol^{-1}, respectively. The overall propagation step consists of the two consecutive steps of addition and fragmentation (Scheme 1). These relatively low values suggest that the addition step is more important than the fragmentation step in determining the propagation rate [12,21]. The value of A_t at low conversion is typically of the order 10^9 L/(mol s) [15,22], resulting in $A_p=7.0\times10^8$ and 2.4×10^6 L/(mol s) for **3** and **4**, respectively, which are typical values for a free radical addition reaction. The addition step being relatively slow in comparison with fragmentation may be interpreted in terms of

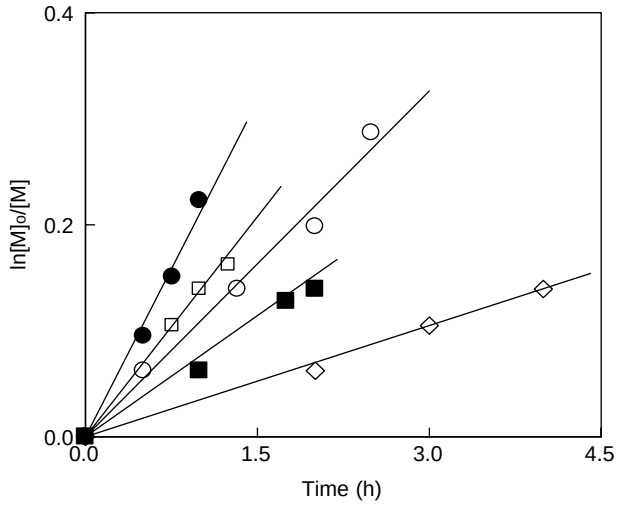

Fig. 7. First-order plots for the polymerization of benzene solutions of **3** at 40 (◇), 50 (■), 60 (○), 65 (□) and 70 (●) °C, where $[M]_0=2$ M, and $[AIBN]_0=0.30$, 0.08, 0.05, 0.02 and 0.02 M, respectively.

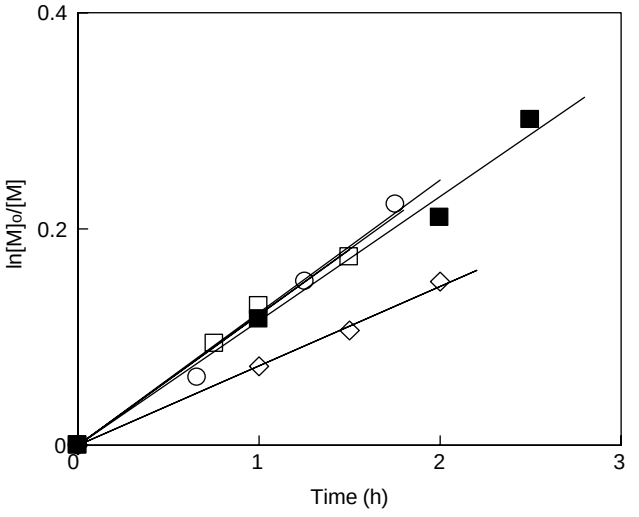

Fig. 8. First-order plots for the polymerization of benzene solutions of **4** at 40 (◇), 50 (■), 60 (○) and 65 (□) °C, where $[M]_0=2$ M, and $[AIBN]=0.350$, 0.200, 0.025 and 0.010 M, respectively.

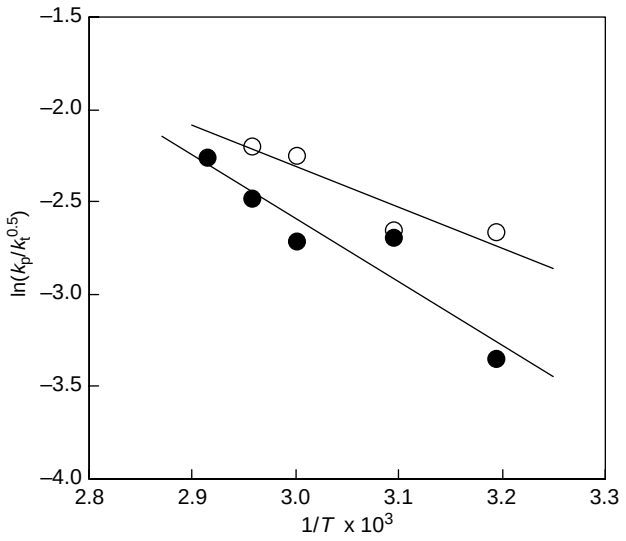

Fig. 9. Plot of $\ln(k_p/k_t^{0.5})$ vs. $1/T$ for the polymerization of 2 M benzene solutions of monomers **3** (●) and **4** (○) at 40–70 °C and 40–65 °C, respectively.

polar and steric effects, i.e. the addition of an electrophilic sulfanyl radical onto a monomer double bond which is in conjugation with an electron-withdrawing acrylate functionality (–COO–) and steric congestion arising from the vinylidene structure.

However, conjugative stabilization of adduct radicals **7** may still make the addition step faster for **1**–**4** in comparison to **5**–**6** containing a non-activated double bond. It is well known that addition of sulfanyl radicals is governed by stability of the formed radical as well as polar effects [23]. For monomer **5**, $(E_p - 0.5E_t) = 72$ kJ mol^{-1} suggests that fragmentation was slower than addition. In contrast the activation energy for **6** $(E_p - 0.5E_t) = 30$ kJ mol^{-1} suggests that the addition step was slower, which can be explained by the two extra remote methyl substituents of this monomer facilitating the fragmentation process [12].

Eight-membered disulfide monomer **5** polymerized approximately 5–6 and 3–5 times faster than **3** and **4**, respectively, and 13–19 times faster than **6** at 40–60 °C [12]. Since **5** is the only one of these monomers where the fragmentation step exerts more influence on the overall propagation rate than the addition step (based on $E_p - 0.5E_t$), it can be inferred that slow addition steps for **3**, **4** and **6** have a large impact on R_p. However, it is difficult to quantitatively relate the differences in R_p with propagation kinetics because one must then assume that all the monomers have identical k_t, and this is debatable owing to differences in steric bulk and viscosity of monomers, as well as differences in the extents of crosslinking as discussed in Section 3.3.

4. Conclusions

Benzene solution polymerizations (2 M) of 7-, 8- and 11-membered lactones **1**, **3** and **4** were carried out at 70, 40–70 and 40–65 °C, respectively. Complete ring-opening up to approximately 25% conversion occurred prior to insoluble polymer formation. The principle cause of insoluble polymer was found to be radical addition onto polymer backbone double bonds resulting in loss of polymer double bonds through crosslinking. ^{1}H NMR showed that **1** had undergone the greatest loss of double bonds with 18% loss at 23% conversion compared with **3** and **4**, which had undergone no more than 5% loss over similar conversion and temperature ranges. The crosslinks were observed by ^{13}C NMR and resulted in a broadening of MWD. However, at higher temperatures (>40 °C for **3** and **4**) adduct radicals formed upon addition to polymer double bonds increasingly underwent fragmentation leading to redistribution of the molecular weights.

Michael adducts of **1** and **3** with 2-methyl-2-propanethiol were prepared in good yields, and demonstrated the location of the CH in ^{13}C NMR spectra, but the lack of this signal in precipitated polymer spectra indicated that hydrogen abstraction by carbon-centred adduct radicals was not significant. Hydrogen abstraction at the allylic position of **1** by propagating sulfanyl radicals is considered to be the main cause of a significantly lower M_n of poly(**1**) compared to poly(**3**) and poly(**4**).

Polymerization rates increased only slightly with increasing ring size. The quantities $(E_p - 0.5E_t)$ and $A_p/A_t^{0.5}$ for **3** and **4** estimated from Arrhenius plots of $k_p/k_t^{0.5}$ showed that addition has a greater influence on the propagation rate than the fragmentation step. Since polymer double bond loss is more prominent than in polymerizations of the disulfides **5** and **6**, one can assume that double bonds of the lactone polymers are more reactive toward radical addition than the disulfides.

Acknowledgements

We thank Science Foundation Ireland for an E.T.S. Walton Visitor Award for Bunichiro Yamada and EPSRC National Mass Spectrometry Service Centre, University of Wales, Swansea for mass spectra.

References

[1] Sanda F, Endo T. J Polym Sci, Part A: Polym Chem 2001;39:265.
[2] Rizzardo E, Evans RA, Moad G, Thang SH. PCT Int Appl 1994 [WO9414792A1 19940707].
[3] Evans RA, Moad G, Rizzardo E, Thang SH. Macromolecules 1994;27:7935.
[4] Evans RA, Rizzardo E. Macromolecules 1996;29:6983.
[5] Evans RA, Rizzardo E. Macromolecules 2000;33:6722.
[6] Evans RA, Rizzardo E. J Polym Sci, Part A: Polym Chem 2001;39:202.
[7] Harrisson S, Davis TP, Evans RA, Rizzardo E. Macromolecules 2001;34:3869.
[8] Harrisson S, Davis TP, Evans RA, Rizzardo E. Macromolecules 2002;35:2474.
[9] Harrisson S, Davis TP, Evans RA, Rizzardo E. Macromolecules 2000;33:9553.
[10] Harrisson S, Davis TP, Evans RA, Rizzardo E. J Polym Sci, Part A: Polym Chem 2002;40:4421.
[11] Phelan M, Aldabbagh F, Zetterlund PB, Yamada B. Macromol Theory Simul 2005;14:109.

[12] Phelan M, Aldabbagh F, Zetterlund PB, Yamada B. Macromolecules 2005;38:2143.
[13] Chaumont P, Asgarzadeh F, Colombani D, Arotcarena M, Baudouin A. Macromol Chem Phys 1998;199:2577.
[14] Tanaka K, Yamada B. Macromol Chem Phys 2000;201:1565.
[15] Buback M, Egorov M, Gilbert R, Kaminsky V, Olaj OF, Russell GT, et al. Macromol Chem Phys 2002;203:2570.
[16] Matsumoto A, Tanaka S, Otsu T. Macromolecules 1991;24:4017.
[17] Zetterlund PB, Yamazoe H, Yamada B. Polymer 2002;43:7027.
[18] Aldabbagh F, Busfield WK, Jenkins ID, Thang SH. Tetrahedron Lett 2000;41:3673.
[19] Lunazzi L, Placucci G, Grossi L. J Chem Sco, Chem Commun 1979;553.
[20] Lunazzi L, Placucci G, Grossi L. Tetrahedron 1983;39:159.
[21] Kobatake S, Yamada B. J Polym Sci, Part A: Polym Chem 1996;34:95.
[22] Beuermann S, Buback M. Prog Polym Sci 2002;27:191.
[23] Ito M, Matsuda M. J Am Chem Soc 1979;101:1815.